A Platinum Open Access Journal for Organic Chemistry

Paper

Free to Authors and Readers

DOAJ Seal

Arkivoc **2021**, part vi, 0-0

to be inserted by editorial office

Conformational control of bis-urea self-assembled supramolecular pH switchable low-molecular-weight hydrogelators

Adam D. O'Donnell,[a] Alexander G. Gavriel,[a] William Christie,[a] Ann M. Chippindale,[a] Ian M. German,[b] and Wayne Hayes[a*]

[a]Department of Chemistry, University of Reading, Whiteknights, Reading, RG6 6DX, U.K.
[b]Kinectrics Inc., 17-18 Frederick Sanger Road, The Surrey Research Park, Guildford, Surrey, GU2 7YD, U.K.
Email: w.c.hayes@reading.ac.uk

Dedicated to Professor Philip Hodge, recognizing his contributions to polymers in synthesis over 45 years

Received mm-dd-yyyy **Accepted Manuscript** mm-dd-yyyy **Published online** mm-dd-yyyy

Dates to be inserted by editorial office

Abstract

We report the synthesis and investigation into the structure-property relationships of eight different low molecular weight hydrogelators based on a bisaromatic urea core unit, all of which form gels as the pH of the solution is lowered. The low molecular weight hydrogelators are functionalized with carboxylic acid moieties on one aromatic ring, and the other aromatic ring features a nitro functional group either in the *meta*- or *para*-position relative to the urea linkage. *Ortho*-methyl substituents were installed on the aromatic rings to enforce a non-coplanar arrangement between the phenyl and urea moieties. Gel formation was triggered by the addition of a mineral acid or the ring-opening hydrolysis of glucono-δ-lactone. The low molecular weight hydrogelators were studied by a variety of analytical techniques, including NMR spectroscopy and rheology. In addition, their ability to uptake a dye, methylene blue, was determined by UV-vis spectroscopy.

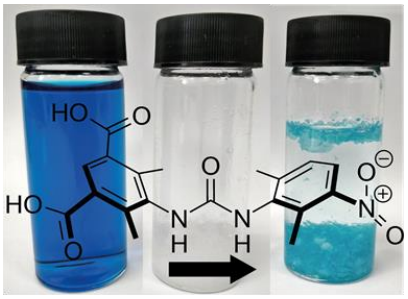

Keywords: Hydrogelator, self-assembly, conformational control

Introduction

A wide range of complex biological assemblies are formed through non-covalent interactions that enable the construction of functional supramolecular structures from low molecular weight building blocks. As such, biomimicry and the understanding of the subtleties of non-covalent interactions are at the forefront of supramolecular self-assembly.[1–4] It is well-known that conformational control is critical in the self-assembly of lipids, folding polypeptides into proteins, and folding nucleic acids into their helical tertiary structure. Aromatic urea systems are ever-present in supramolecular chemistry because of their strong self-assembly through self-complementary hydrogen bonding, and π-π stacking interactions.[5–7] Their synthetic accessibility and strong association characteristics have been exploited to synthesize self-assembled organogelators,[8–10] hydrogelators,[11–13] liquid crystals,[14] self-assembled monolayers,[15] hydrogen-bonded molecular capsules,[16] tunable hydrogen bond-donating catalysts,[17] and supramolecular polymers,[18] as well as in anion complexation,[19] and crystal engineering.[20] Bouteiller and co-workers illustrated the effects of conformation control of aromatic bis-urea systems through viscometry measurements with *ortho*-methyl substituents found to enforce a non-coplanar conformation between the urea and the phenyl moiety, in turn enhancing hydrogen bonding.[21] Substitution of the *ortho*-position with methyl groups was shown to be more effective at increasing the viscosity of the solution than larger functional groups, resulting from reduced steric hindrance allowing for rotation. Low-molecular-weight gelators (LMWG) have invited investigation for several reasons; they offer a unique opportunity to design soft materials with controllable assembly through structural modification of the associating groups and have found applications ranging from biomedical injectable gelators designed to release a drug molecule at its desired location,[22] to removing pollutants from wastewater or organic solvents.[23,24] Adams and co-workers analysed an Fmoc-dipeptide LMWG and found that the mechanical properties of the gels prepared were dependent on the volume fraction of the co-solvent and the temperature cycle used to generate the gel.[25] Smith and co-workers developed a hybrid gel by combining two supramolecular gelators, one of which enabled the controlled release of an active pharmaceutical ingredient and the other provided enhanced mechanical stability.[26] Ulijn and co-workers investigated the significance of the Fmoc moiety in aromatic peptide amphiphile hydrogelators and concluded that the Fmoc moiety provided a rigid linker of sufficient length to allow for effective assembly.[27] In this paper, we report the synthesis of eight bisaromatic ureas and the investigation of the structure-property relationships of these low molecular weight hydrogelators with relevance to applications such as water purification.

Results and Discussion

A series of potential low molecular weight aromatic urea hydrogelators were designed and synthesized (see **1 – 8** in Figure 1, see the Supporting Information (SI) file, Figures S1 – 42 for the characterization data of these compounds and their precursors **9** – **20**).

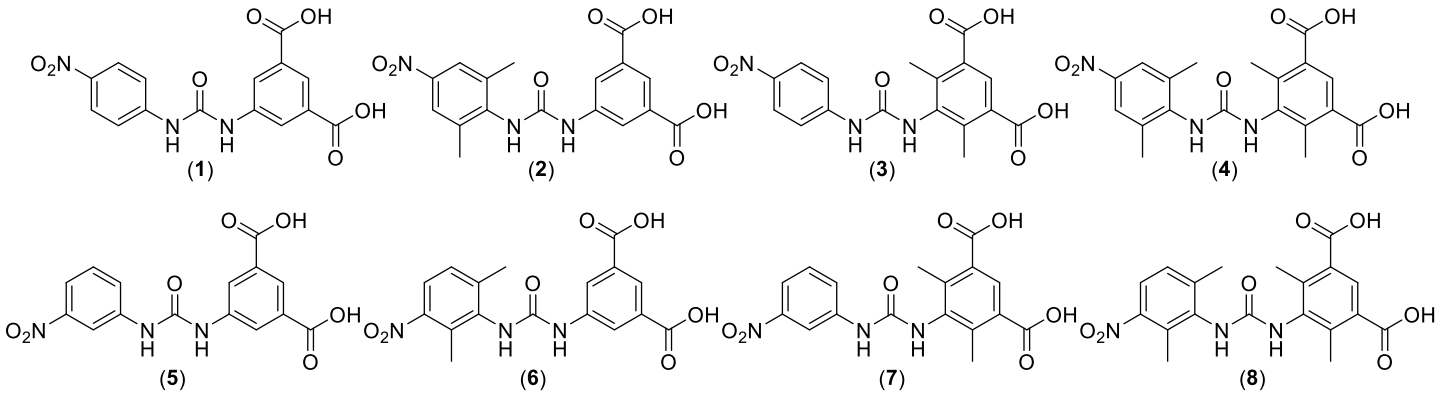

Figure 1. The bisaromatic ureas (**1** – **8**) that were designed, synthesized, and investigated in this study. **1** and **5** have previously been reported by Hayes and co-workers.[13]

Synthesis

The synthesis of bisaromatic ureas featuring *ortho*-methyl substituents required the generation of the corresponding aniline precursors. Chloromethylation of *meta*-xylene with HCl and paraformaldehyde in the presence of acetic acid afforded 1,5-bis(chloromethyl)-2-4-dimethylbenzene **9** (Scheme 1).[28] A modified procedure from Hopff *et al.*[29] was used to nitrate selectively *ortho*- to the methyl substituents (to yield **10**, see the solid-state structure in the SI, Figure S41) and then oxidize the chloromethyl substituents to carboxylic acids (**11**). ^{1}H NMR spectroscopic analysis of the diacid **11** revealed the disappearance of the methylene resonance at δ_H 4.86 ppm and the appearance of a broad singlet at δ_H 13.56 ppm corresponding to the carboxylic acid protons (see SI, Figure S21). Furthermore, Fourier-transform infrared (FTIR) spectroscopic analysis of **11** revealed a strong absorbance band at 1668 cm^{-1} corresponding to the aromatic carboxylic acid stretch. Esterification with thionyl chloride and methanol yielded the desired dimethyl isophthalate **12** in excellent yield (see the solid-state structure in the SI, Figure S42). Selective reduction of the nitro functional group with hydrogen and Pd/C in MeOH to an arylamine (**13**) was confirmed by ^{1}H NMR spectroscopic analysis (see SI, Figure S25), which featured a broad singlet at δ_H 5.09 ppm. Subsequent ester hydrolysis was achieved with NaOH was monitored by thin-layer chromatography (TLC); following completion, the solvent was removed, and the aminoisophthalic acid **14** was isolated by acidification with HCl until pH = 4, at which point the desired amine precipitated.

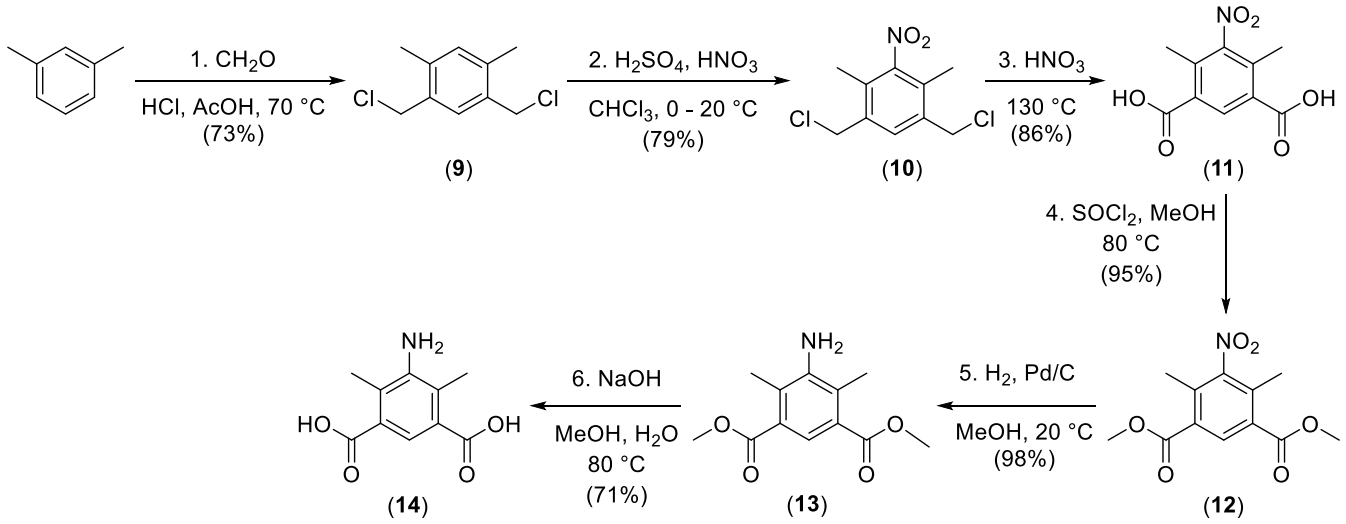

Reagents and conditions: 1. CH_2O (2.3 equiv), HCl, AcOH, 70 °C, 96 hours, 73%. 2. H_2SO_4, HNO_3, $CHCl_3$, 0 – 20 °C, 1 hour, 79%. 3. HNO_3, 130 °C, 24 hours, 86%. 4. $SOCl_2$ (5.0 equiv), MeOH, 80 °C, 6 hours, 95%. 5. H_2, Pd/C (10 wt. %), MeOH, 20 °C, 3 hours, 98%. 6. NaOH (3.0 equiv), MeOH, H_2O, 80 °C, 5 hours, 71%.

Scheme 1. Synthesis of 5-amino-4,6-dimethylisophthalic acid (**14**).

The *ortho*-methyl-substituted isocyanates **15** and **16** were synthesized from their respective amines **17** and **18** using phosgene in toluene and isolated in excellent yields (> 99%) (see Scheme 2). In the case of the isocyanate **15** featuring a nitro group *meta* to the reactive isocyanate unit, this was synthesized from 2,6-dimethylaniline. Nitration of 2,6-dimethylaniline afforded the desired 2,6-dimethyl-3-nitroaniline **17** in 83%. A more complex approach was required to generate the *para*-nitro substituted isocyanate **16**. 2,6-Dimethylaniline was first converted to the corresponding toluenesulfonamide **19** to direct nitration *meta* to the methyl groups, yielding **20**. Treatment of the *para*-nitro-toluenesulfonamide **20** with sulfuric acid afforded the desired *para*-nitroaniline **18** in 81%. A strong absorbance band confirmed isocyanate generation at 2272 and 2263 cm^{-1} in the IR spectra of **15** and **16**, respectively, and also by the $^{13}C\{H\}$ NMR spectra (broad quaternary carbon resonances evident at δ_C 124.8 and 125.7 ppm, respectively).

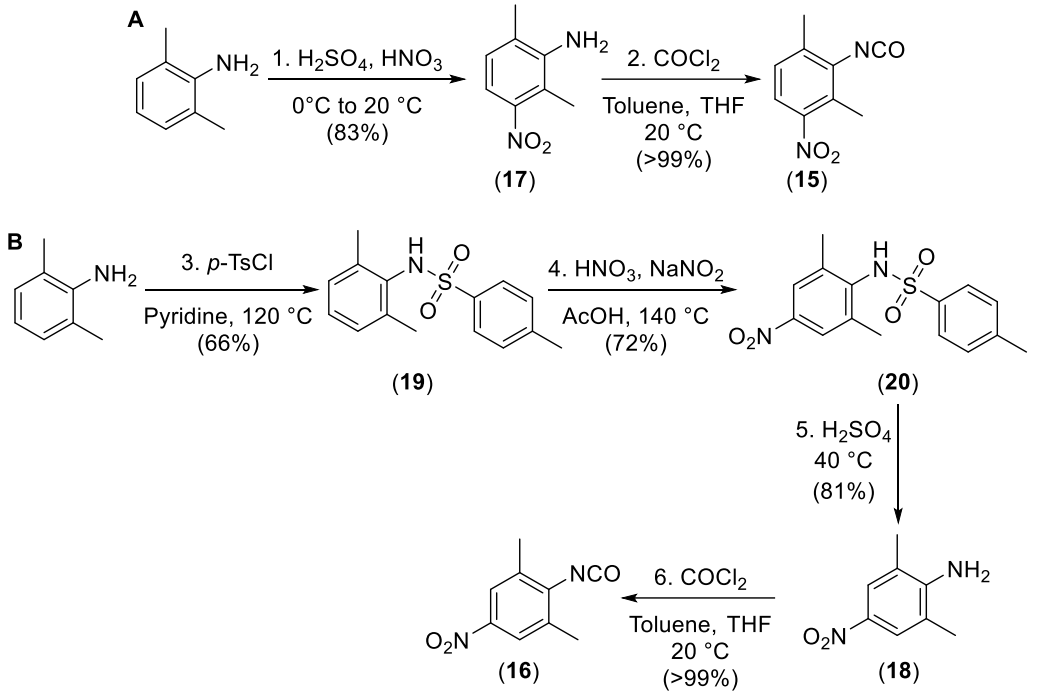

Reagents and conditions: **A)** 1. H_2SO_4, HNO_3, 0 – 20 °C, 1 hour, 83%. 2. $COCl_2$ (5.0 equiv, 15.0 wt. % in toluene), THF, 20 °C, 12 hours, > 99%. **B)** 1. *p*-TsCl, pyridine, 120 °C, 4 hours, 66%. 2. HNO_3, $NaNO_2$, AcOH, 140 °C, 2 hours, 72%. 3. H_2SO_4, 40 °C, 12 hours, 81%. 4. $COCl_2$ (5 equiv, 15 wt. % in toluene), THF, 20 °C, 12 hours, >99%.

Scheme 2. The synthesis of the isocyanates **15** and **16**.

Ureas **1 – 8** were then synthesized by reacting the respective amine 5-aminoisophthalic acid (**21**), or **14** with the appropriate isocyanate 3-nitrophenylisocyanate (**22**), or 4-nitrophenylisocyanate (**23**) (see Scheme 3). The reactions were monitored with FTIR spectroscopy to study the consumption of the isocyanate group and conversion to the corresponding urea.

15, **16**, **22**, **23** **14**, **21** **1 - 8**

14: $R_5 = R_6 = CH_3$
15: $R_1 = R_2 = CH_3$, $R_3 = NO_2$, $R_4 = H$
16: $R_1 = R_2 = CH_3$, $R_3 = H$, $R_4 = NO_2$
21: $R_5 = R_6 = H$
22: $R_1 = R_2 = H$, $R_3 = NO_2$, $R_4 = H$
23: $R_1 = R_2 = H$, $R_3 = H$, $R_4 = NO_2$

1: $R_1 = R_2 = R_3 = H$, $R_4 = NO_2$, $R_5 = R_6 = H$
2: $R_1 = R_2 = CH_3$, $R_3 = H$, $R_4 = NO_2$, $R_5 = R_6 = H$
3: $R_1 = R_1 = R_2 = R_3 = H$, $R_4 = NO_2$, $R_5 = R_6 = CH_3$
4: $R_1 = R_2 = CH_3$, $R_3 = H$, $R_4 = NO_2$, $R_5 = R_6 = CH_3$
5: $R_1 = R_2 = H$, $R_3 = NO_2$, $R_4 = R_5 = R_6 = H$
6: $R_1 = R_2 = CH_3$, $R_3 = NO_2$, $R_4 = R_5 = R_6 = H$
7: $R_1 = R_2 =H$, $R_3 = NO_2$, $R_4 = H$, $R_5 = R_6 = CH_3$
8: $R_1 = R_2 = CH_3$, $R_3 = NO_2$, $R_4 = H$, $R_5 = R_6 = CH_3$

Scheme 3. The general synthetic protocol used to afford the bisaromatic ureas **1** – **8**.

Critical gelation concentration discussion

The gel-forming potential of the bisaromatic ureas was assessed initially using vial inversion and the HCl pH switching methods (see SI, Figures S43-47). All eight of the gelators were soluble in basic solution (NaOH, 0.1M) and upon acidification either formed a free-standing gel or failed to be self-supporting. The bisaromatic ureas **1** and **5** each exhibited the same critical gelation concentrations (CGC) as reported previously (see Table 1).[13] Unexpectedly, **2** did not produce a free-standing gel upon pH switching and instead yielded a weak gel that did not pass the vial inversion test up to a gelator concentration of 20 mM (see Figure S43). Gelator **3** also did not pass the vial inversion test and instead formed a granular precipitate upon pH switching over the concentrations tested (see Figure S43). The only structural difference between the bisaromatic ureas **1**, **2,** and **3** is the presence of the two *ortho*-methyl substituents on **2** and **3**. The precipitation of bisaromatic urea **3** indicates increased structural order and phase separation from the solvent. Previously we have observed in a structurally related bisaromatic urea series that precipitation also occurs for structures where the nitro group is not present, highlighting its importance in mediating hydrogen bond formation and fibril assembly in the gel state.[13] Solid-state analysis has shown that hydrogelator **1** assembles as a regular array of ribbons with planar molecules connected via urea to nitro hydrogen bonds and dimerization of the carboxylic acid functional groups.[12] It is evident from the comparison of bisaromatic ureas **1 – 3** that the addition of *ortho*-methyl substituents to the aromatic units on either side of the urea has had a disruptive effect on the gel assembly process, probably by twisting the aromatic rings perpendicular to the urea and preventing co-planar assembly. Upon comparing the infrared spectroscopic data, the absorption band associated with the urea carbonyl was shifted to higher wavenumbers, 1645 and 1641 cm^{-1} for **2** and **3**, respectively, corresponding to the free urea carbonyl, in comparison to **1** (1600 cm^{-1}), indicative of an ordered hydrogen bonded urea carbonyl. The nitro group in **1** is a hydrogen bond acceptor able to effectively disrupt urea-urea hydrogen bonding in preference for urea-nitro interactions and form a regular array of ribbons;[7] however, in **2** and **3**, urea-urea interactions are now promoted due to the conformational control exerted by the *ortho*-methyl substituents.[21] This mismatch of intramolecular interactions is the likely reason for the inability of both **2** and **3** to form robust gel networks under comparable conditions to the bisaromatic urea **1**. This mismatch of intramolecular interactions was also evident for bisaromatic urea **4**; however, there is now an increased preference for urea-urea interactions as the urea is now fixed into its perpendicular conformation. As a result, the urea carbonyl stretch was observed at 1614 cm^{-1} and weak gels could be formed (CGC of 3.3 mM). By employing the HCl pH switching procedure, the CGC values were established between 0.9 and 6.5 mM for the six gel-forming bisaromatic ureas (**1, 4 – 8**) (see SI, Figures S43-47). As a result of the low molecular weights of these compounds and their ability to form stable gels below 1% wt %, all six can be categorized as "super gelators".[30]

Table 1. CGC values for hydrogelators synthesized in this study as determined by pH switching with HCl.

Compound	**(1)**	**(2)**	**(3)**	**(4)**	**(5)**	**(6)**	**(7)**	**(8)**
CGC (mM)	0.9	Not observed	Not observed	3.3	4.5	6.5	2.4	3.3

Rheological Studies

Rheological measurements were conducted at a constant gelator concentration (20.0 mM) to examine the viscoelastic properties of the self-assembled hydrogels. Gelation kinetics were initially assessed by oscillatory time sweep experiments using the robust glucono-δ-lactone protocol introduced by Adams *et al.* to slowly switch the pH of the solution whilst simultaneously measuring storage and loss modulus as a function of time (Figure 2A).[31] As the pH was lowered, fibers form and eventually network formation became apparent

entrapping the water medium. After equilibrating for twelve hours, the most stable hydrogelators (**1**, **4**, **6**, **7**) were subjected to amplitude (Figure 2B) and frequency sweep experiments (Figure 3).

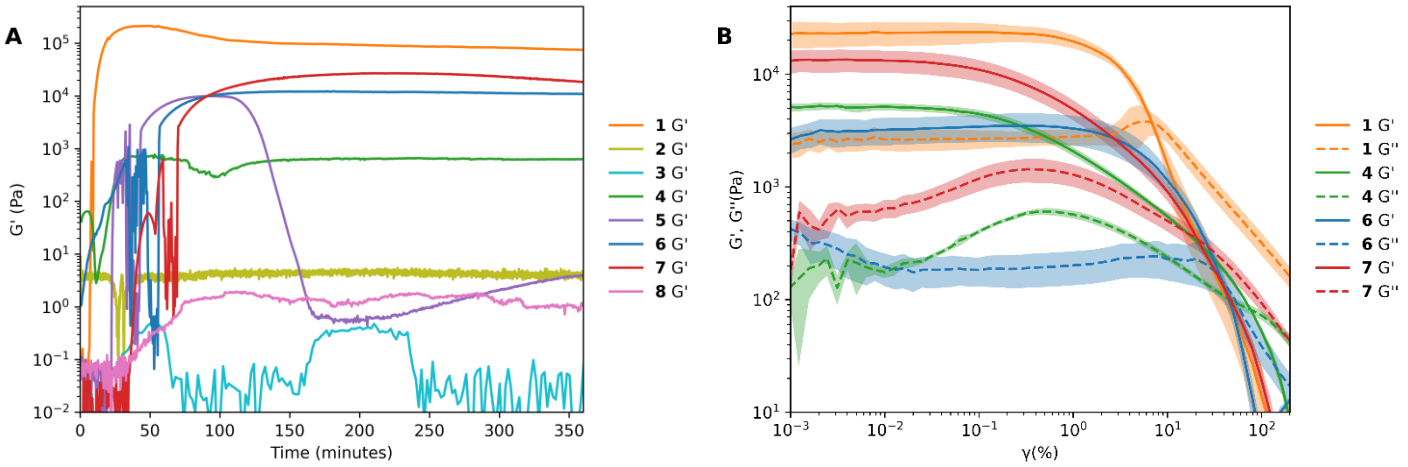

Figure 2. A) Storage modulus *vs*. time graphs for hydrogels formed from gelators **1 – 8** as the pH was slowly switched using glucono-δ-lactone. **B)** Strain-controlled oscillatory amplitude sweep of hydrogelators (**1**, **4**, **6**, and **7**), from 0.001% to 100% shear strain, shaded regions are standard deviation error bars calculated from three separate measurements.

Hydrogelator **1** proved to be the most robust gelator network in all of these tests, and its maximum storage modulus was observed within an hour of the addition of glucono-δ-lactone (Figure 2A). The appearance of a plateau, followed by a slight drop, indicates an equilibration period and after which the storage modulus remains approximately constant. The storage modulus of the hydrogelator **5** reached its maximum 100 minutes after the addition of glucono-δ-lactone. A gel to crystal transition was observed at this point, resulting in a steep drop in the gel's storage modulus and syneresis of the entrapped water. A similar gel to crystal transition was observed for **7**; however, the steep drop in storage modulus was not observed, and the partial gel phase is seen to be stable in oscillatory time sweep measurements. Hydrogelator **6** exhibited a very visually similar gel phase to that of **1**; a transparent gel is formed, which does not appear to undergo the same gel to crystal transition seen in the **5** and **7**. The position of the *ortho*-substituents has a significant impact on the gel assembly. Hydrogelator **4** went through a gel to crystal transition within 12 hours of pH switching and remained stable after that. Hydrogelator **8** underwent a shallow increase in storage modulus as the solution became more acidic. The hydrogel formed from **8** is several orders of magnitude weaker than those of the other hydrogelators, and the gel robustness was thus not evaluated in greater detail. Both the bisaromatic ureas **2** and **3** failed to form gel networks and preferred to precipitate upon pH switching with glucono-δ-lactone. Oscillatory amplitude sweep experiments were performed to determine the yield stress, yield strain, and yield strain at the inversion of G' and G'' (Table S5). Frequency sweep experiments were performed under a constant strain of ($\gamma = 0.1\%$), and it was observed that the storage modulus (G') is almost independent of angular frequency within the tested frequency range and that the storage modulus (G') is approximately an order of magnitude greater than the loss modulus (G''), confirming the presence of the gel phase (Figure 3B).

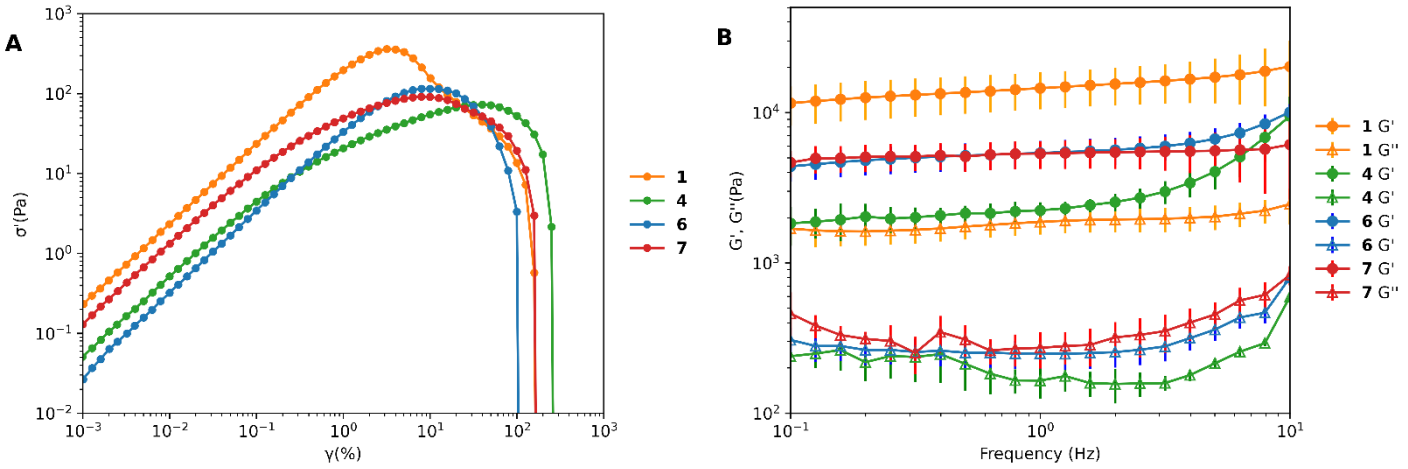

Figure 3. A) Strain-controlled oscillatory amplitude sweep to measure elastic stress as a function of applied strain for hydrogels **1**, **4**, **6**, **7**. **B)** Frequency sweep experiments showing the parallel dependence of G' and G'', standard deviation error bars were calculated from three separate measurements.

Microscopic self-healing behaviour was probed for the urea-based hydrogelator networks via rheological step strain measurements.[32–37] Mesoscale ruptures are induced at high shear strain, a critical parameter for the processing and injection of soft materials. As shown in Figure 4, a high strain oscillatory shear strain sweep (γ = 250%, frequency = 1 Hz, 250 s) resulted in a quasi-liquid structure (G">G') because of the structural breakdown of the gel induced at high shear and the hydrogel material can thus flow. Upon removing the subjected high shear strain and applying a low magnitude strain sweep (γ = 0.1%, frequency = 1 Hz, 250 s), the network reforms, G' recovers its initial value to form a quasi-solid state following the stress-induced flow. The rate and extent to which **1**, **4**, and **7** recovered their initial state were effectively identical over several cycles of breaking and reforming the network, highlighting the reversible and robust nature of these dynamically cross-linked networks. Reversible dissociation and re-association of the network can effectively retard network failure, prolonging the material's lifespan. Most interestingly, the hydrogel network formed from gelator **6** did not recover its initial state upon returning to a low shear strain (γ = 0.1%) and formed a gel network an order of magnitude less robust than the initial gel. Upon closer inspection, when applying a high shear strain, mesoscale ruptures result in network destruction. Almost immediately, a gel network was reformed within this high shear domain where G' exceeds G'' by an order of magnitude. This resulted in slower network formation upon removal of the shear strain, evidenced by the steep gradient of G' and G'' and by a reduction in G' by a factor of 31 relative to that recorded before the high-shear exposure. Intrigued by this phenomenon, further rheological studies were conducted, and the hydrogelator **6** was able to recover its initial G' property following an extended low shear recovery period of 1200 s (See Figure S48).

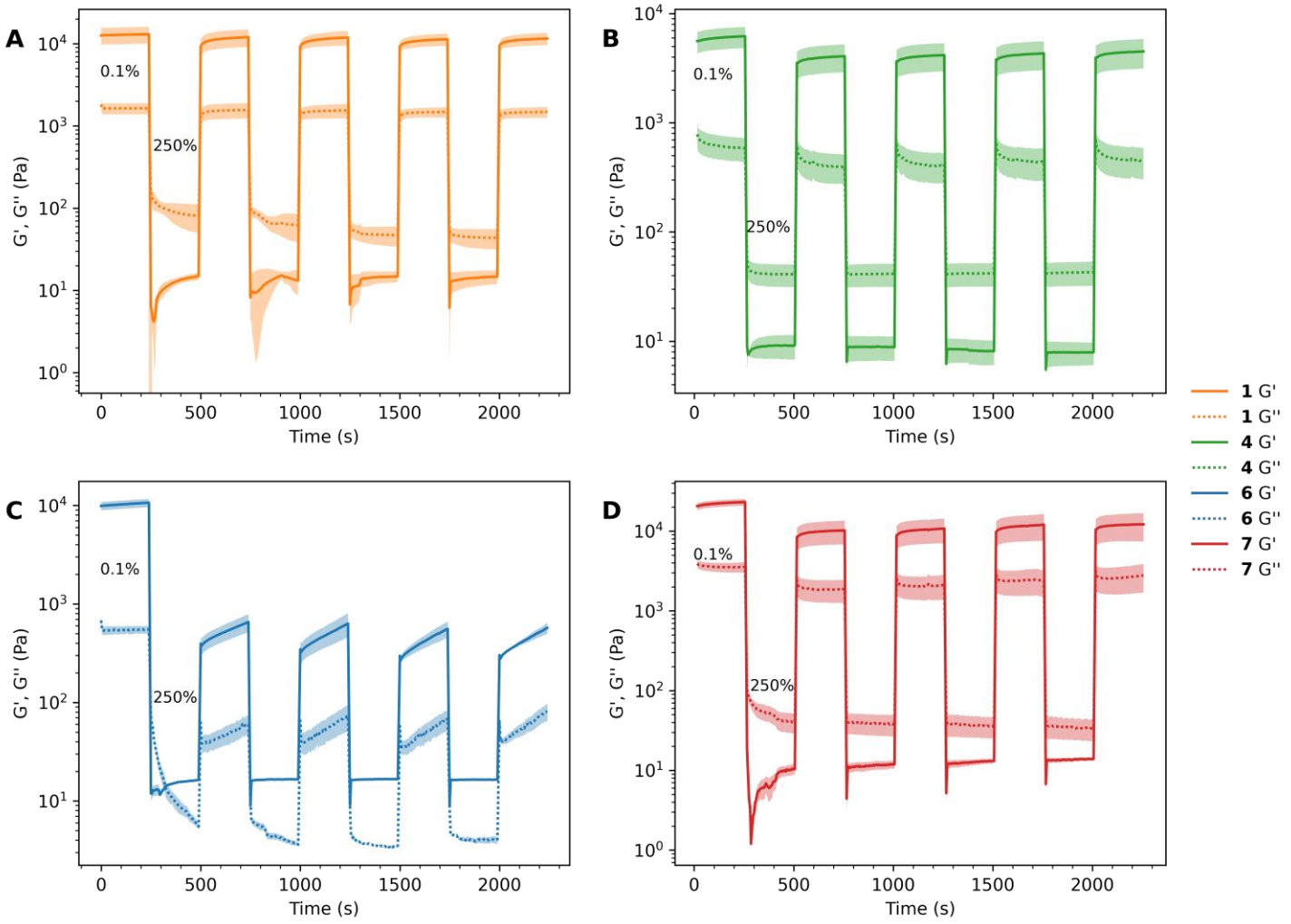

Figure 4. Continuous step-strain measurements of **A) 1**, **B) 4**, **C) 6**, and **D) 7** hydrogelator networks at 25 °C (high-amplitude oscillatory parameters: strain γ = 250%, frequency = 1 Hz, low-amplitude oscillatory parameters: strain γ = 0.1%, frequency = 1 Hz). Shaded regions are standard deviation error bars calculated from three separate measurements.

NMR Spectroscopic Kinetic Studies

The gel assembly kinetics were also probed by ^{1}H NMR spectroscopy.[38] Before gel assembly, the gelator molecules are sufficiently mobile to be detected on the NMR timescale; they have suitable relaxation times for NMR spectroscopic analysis. As the pH is switched the gel formation occurs, the non-mobile gel fibers become invisible to the spectrometer because of their molecular size and slow diffusion characteristics. Monomeric and oligomeric units can be quantified against an internal standard, in this case, dimethylsulfoxide (DMSO), by integrating the regions associated with the mobile phase. Kinetic information can be obtained by monitoring the changes in the ^{1}H NMR spectrum over time following the addition of glucono-δ-lactone. By plotting the concentration of gelator molecules in the mobile phase against time, it was evident that there was a rapid initial drop in concentration in the first 20-30 minutes after addition (See Figure S 49). This can be attributed to the rapid conversion of glucono-δ-lactone into gluconic acid by residual NaOH, rapidly lowering the pH of the solution. Afterwards, there is a buffering period as the pH gradually lowers to the pK_a of the gelator; this can be seen as a plateau in the concentration *vs*. time plot (See Figure S 49). Once the pH is equivalent to the pK_a of the gelator, assembly of the LMWG network proceeds over several hours. The presence of methyl groups *ortho*

to the carboxylic acids of the hydrogelators lowers their pKa, illustrated in a series of regioisomers by the increased buffering period of **3** and **7** relative to **2** and **6,** respectively. Thus, hydrogelators **3** and **7** took up to 750 minutes to convert to the less mobile phase compared to less than 250 minutes for both **2** and **6**. Intriguingly, the influence of the *ortho*-methyl substituents on the pK_a of carboxylic acids of **4** and **8** is not reflected as significantly in the buffering period. Rationalizing this difference is not trivial, as the apparent pK_a of gelator molecules is dependent on the self-assembly step and can effectively change the pK_a from what might be expected for the non-assembled small molecule.[39] As such, this decreased buffering period was attributed to increased order within the gel network, imposed by the conformation control of the urea phenyl torsion predicted to accommodate two methyl groups *ortho* to the urea on each aryl ring. It is proposed that the urea-urea interactions dominate and consequently increase the apparent pK_a of **4** and **8**. To further understand the nature of the assembly, the data were then fitted to Avrami's kinetic model,[40] where *n* is the Avrami exponent and reflects the growth of the hydrogelator network. Exponent values close to 1.0 are associated with 1-dimensional growth with little branching, whereas values of 2 or higher are associated with 3-dimensional growth and branching. The effect is demonstrated elegantly by hydrogelators **2** and **8,** which have exponents of 1.0, and in the case of **2** a stable gel network could not be formed when pH switching with glucono-δ-lactone (Figure 2A); similarly, **8** formed one of the weakest gel networks as determined by rheological testing. Hydrogelator **3** exhibited the most 3-dimensional growth, and an Avrami exponent value of 2.28 was determined for this compound, indicating significant branching and eventual precipitation from solution rather than gel formation. Gelators **4**, **5,** and **7** all have exponents between 1.6 and 1.9, suggesting branching, and tended to undergo gel to crystal transitions over time as the extended network formed. Hydrogelators **1** and **6** had exponents between 1.33-1.38, suggesting some degree of branching, exhibited metastability,[41,42] and did not undergo observable gel to crystal transitions for periods greater than one month, illustrating the requirement for understanding the delicate balance in network growth when designing gelator molecules.

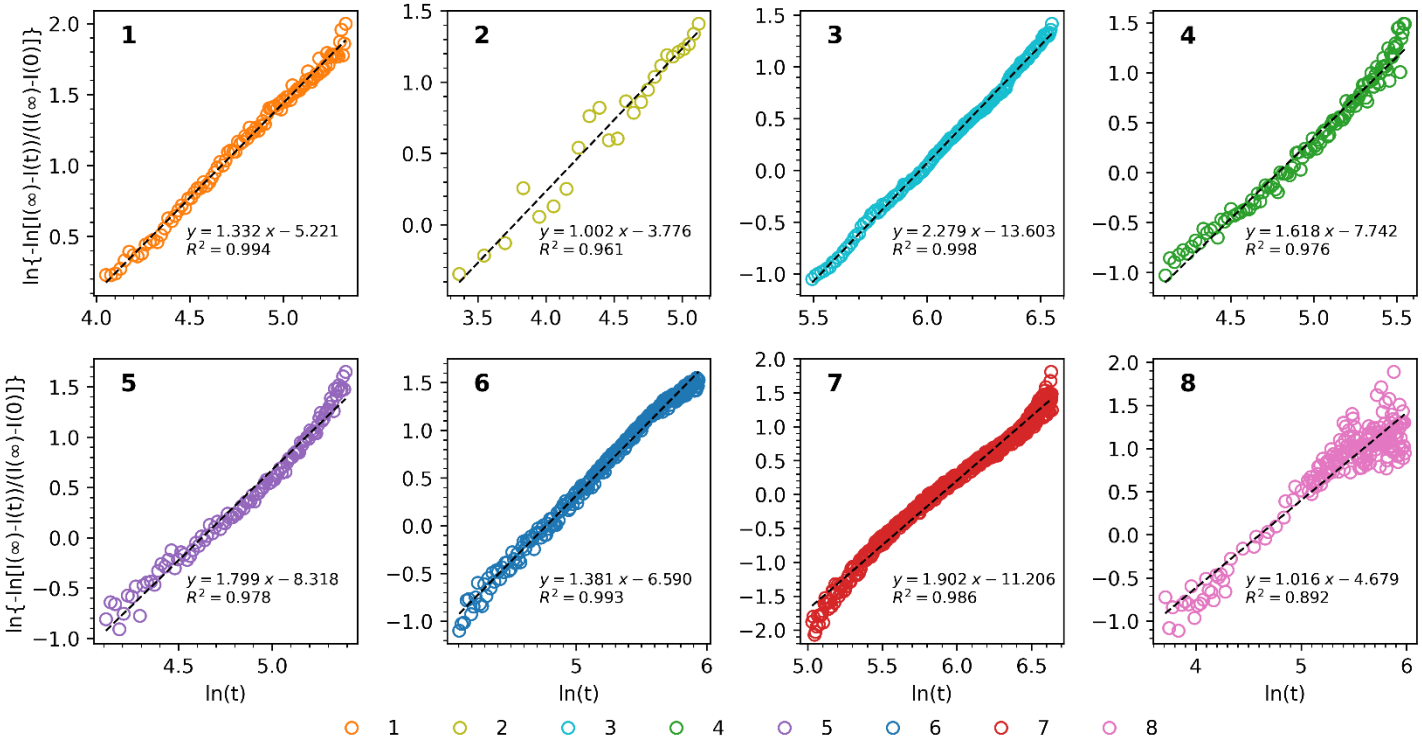

Figure 5. Avrami plot for the network formation of gelators **1 – 8** (20 mM) as monitored by ^{1}H NMR spectroscopy, where the Avrami exponent, *n*, is the gradient of the line of best fit.

Dye uptake experiments

Organic dyes such as methylene blue have been used as model organic pollutants because their UV-vis absorbance characteristics enable the prediction of contaminant removal from water sources by gel media.[17] Previous studies have shown that the hydrogel formed from bisaromatic urea **1** is an effective scavenger of methylene blue, methylene green, and Rhodamine B.[13] In this study, it was decided to reduce the quantity of hydrogelator used from 1.00 mL of gel (concentration: 20 mM) to 0.25 mL (with a concentration of 10 mM) to conduct dye uptake studies within a cuvette. The gelators were pH switched using HCl with the resultant solution left to stand without agitation, thus removing the influence of mixing. The dye, in this case, methylene blue (3.00 mL, 4.0 mgL^{-1}), was pipetted gently onto the gel surface, allowing dye sequestering. Interestingly, it was found that four of the eight hydrogelators (**1**, **5**, **6**, and **8**) were able to effectively sequester the planar cationic dye from the solution (Figure S 50), evident by the significant drop in absorbance (Figure 6 and SI Figure S51). Hydrogelators **2** and **3** showed poor dye sequestering ability and did not form stable gels when pH switching with glucono-δ-lactone. Hydrogelator **5** precipitated after pH switching with HCl, and although it showed impressive extraction capabilities (88%), it was not suitable for effective dye extraction. Hydrogelator **6** proved to be more stable than **5** and **7** and had a similar dye extraction capability (94%) to **1** (95%) and **8** (96%). Hydrogelators **4** and **7** showed a reduced proficiency at removing methylene blue from solution with only 54% and 46% of the methylene blue removed, respectively. The asymmetry of the aromatic rings in **7** in comparison to **8** may result in a less planar network, potentially presenting a barrier to methylene blue intercalation and reducing its extraction from solution.

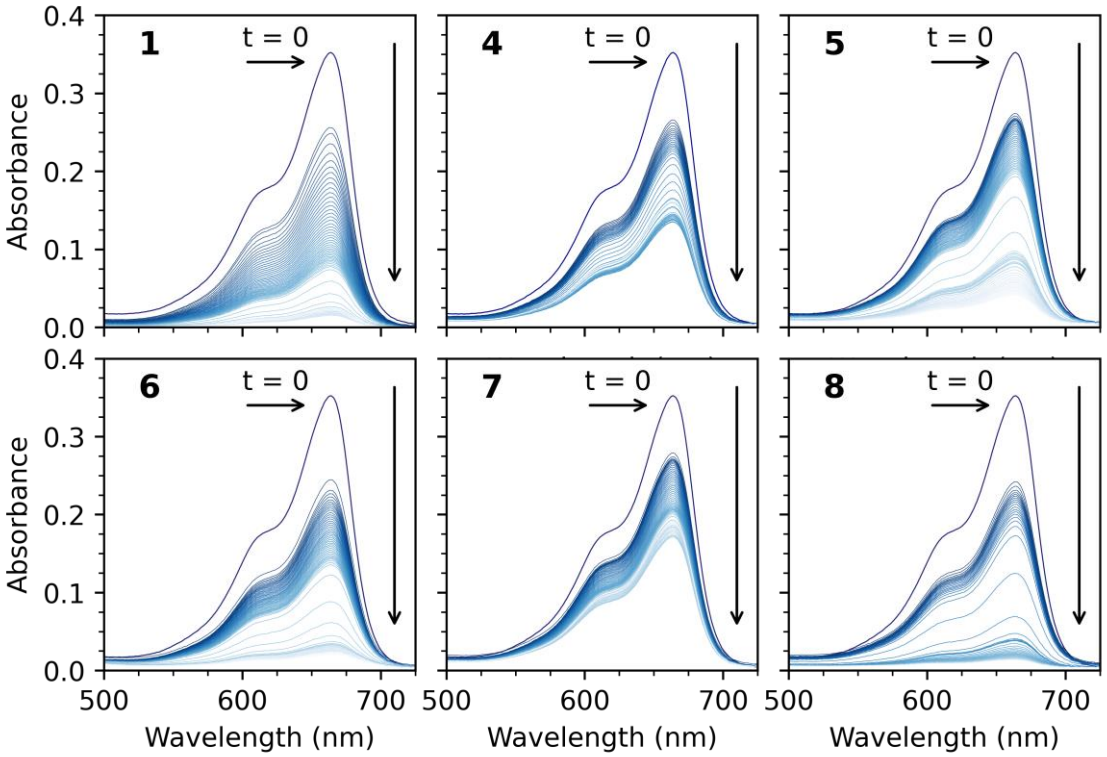

Figure 6. Plot of methylene blue absorption for hydrogelators **1**, **4**, **5**, **6**, **7**, and **8**; each line represents a measurement taken every hour.

Conclusions

A library of structurally similar bisaromatic ureas (**1 – 8**) were synthesized and characterized. The gelation of these behaviour compounds was investigated in aqueous media by acidifying a basic solution of the hydrogelator by either the addition of HCl or by the slow hydrolysis of glucono-δ-lactone. Gel assembly kinetics were monitored using rheology by ^{1}H NMR spectroscopic analysis; rheological measurements also assessed the gel's ability to form stable networks and reform after experiencing destructive oscillatory shear. The bisaromatic ureas **1**, **6** and **8** were more effective at extracting methylene blue from the solution. This was attributed intermolecular urea to nitro interactions promoting the formation of a 1-dimensional network (as determined by Avrami plots) thus allowing for the intercalation of the planar cationic dye. In contrast, the bisaromatic ureas **4** (54%) and **7** (46%) which featured *ortho*-methyl groups formed weak gel networks and were not suitable for dye sequestering - the result of the domination of urea-urea associations as an interaction mode for those structures. In addition, although bisaromatic urea **5** did exhibit excellent dye extraction capabilities (88%), it underwent a gel to crystal transition if left for greater than twelve hours and therefore is not practical for dye extraction. The structure-property relationships developed in this study will contribute to improvements in the targeted design of materials for highly effective water purification systems.

Experimental Section

General. Dry dimethylformamide (DMF) (Sigma Aldrich) was used as supplied. Tetrahydrofuran (THF) was distilled from benzophenone and sodium before use. All other reagents were purchased from Sigma Aldrich and used as received. Thin-layer chromatography (TLC) was conducted using TLC silica gel 60 F254 aluminum-backed sheets (Sigma Aldrich) and visualized with ultraviolet light, ninhydrin, or potassium permanganate staining. ^{1}H NMR and ^{13}C{H} NMR spectra were recorded on either a Bruker Nanobay 400 or a Bruker DPX 400 spectrometer operating at 400 MHz for ^{1}H NMR or 100 MHz ^{13}C{H} NMR, respectively. The data were processed using MestReNova Version 11.0.3-18688. Samples for NMR spectroscopic analysis were prepared in $CDCl_3$ or DMSO-d_6, and dissolution was aided with brief heating. Chemical shifts (δ) are reported in ppm relative to tetramethylsilane (δ 0.00 ppm) for $CDCl_3$ and the residual solvent resonance (δ 2.50 ppm) for d_6-DMSO in ^{1}H NMR. Infrared (IR) spectroscopic analysis was carried out using a Perkin Elmer 100 FT-IR (Fourier Transform Infrared) instrument with a diamond-ATR sampling accessory. Ultraviolet-visible spectra were measured with a Varian Cary 300 spectrophotometer, using 1 cm^2 quartz cuvettes, in the wavelength range 500–750 nm. Mass spectrometry was conducted using ThermoFisher Scientific Orbitrap XL LCMS. The sample was introduced by liquid chromatography, and sample ionization was achieved by electrospray ionization (ESI). Melting points were recorded using a Stuart MP10 melting point apparatus and are uncorrected. Elemental microanalyses of **3**, **8**, **9** **10**, **14**, **15** and **16** were performed by MEDAC Ltd. Rheological measurements were performed on a Malvern Kinexus Lab+ rheometer using a 40 mm diameter 4° cone and plate geometry configuration or a 20 mm parallel plate geometry and analyzed using RSpace Kinexus v1.75.2326 software.

Dye adsorption studies

Dye uptake was measured using 1 cm^2 quartz cuvettes with a 20 mM solution of each hydrogelator in a 0.1 M NaOH solution. 125 µL of this solution was then pipetted into the base of a cuvette to which HCl (125 µL, 0.2 M) was added to switch the pH and initiate gelation. A stock solution of methylene blue (3.00 mL, 4.0 mgL^{-1}) was then pipetted carefully on top of the gel. Scans were performed once a minute with the spectrometer operating in kinetic mode.

pH switching procedures

The bisaromatic ureas were subject to two different pH switching methodologies. In both cases, the dried hydrogelator was dissolved in 0.1 M NaOH solution and briefly sonicated to ensure complete dissolution. The pH of the solution was then switched using either aliquots of 0.2 M HCl (and left momentarily to equilibrate) or alternatively two equivalents of glucono-δ-lactone were added as a solid and vortexed until complete dissolution had occurred.

Critical gelation concentration determination

Critical Gelation Concentration (CGC) determination was carried out in a 2 mL screw-top glass vial. The minimum gelator mass was determined to the nearest milligram and varied every 0.2 mg to obtain an accurate CGC value.

NMR gelation kinetic measurements

Using the glucono-δ-lactone pH switching procedure, which induces a controlled change of the solution's pH, the gelation kinetics can be measured.[31] The gel-phase is invisible to the spectrometer, and the concentration of sol-phase can be measured against an internal standard, in this case, non-deuterated DMSO.[38] Fitting Avrami's kinetic model to the concentration *vs*. time data,[40] the Avrami exponent of n was determined. This analysis was performed on all of the bisaromatic ureas (**1 – 8**).

Rheology measurements

Oscillatory time sweep measurements involved casting 1000 µL of 20 mM solutions of **1 – 8** prepared according to the gel pH switching method described above onto the stainless-steel plate and then lowering the cone to the measurement position (0.15 mm). Oscillatory time sweep gelation measurements commenced immediately after that, but otherwise, the solution was left to form a gel for 12 hours. A temperature of 25 °C was used for the oscillatory time sweep study, frequency, and amplitude sweeps. Oscillatory time sweep experiments were performed at 1 rad/s and constant strain (γ) = 0.1%. Frequency sweeps were performed with a log ramp frequency (f) = 0.01 – 10 Hz and constant strain (γ) = 0.1%. Amplitude sweeps were performed with constant frequency (f) = 1 Hz and log ramp strain (γ) = 0.1 – 100%. Thixotropy measurements were performed alternating between low strain (f = 1 Hz, γ = 0.1%, 250 s) and high strain (f = 1 Hz, γ = 250%, 250 s).

Synthesis of compounds 1, 2, 3, 4, 5, 6, 7 and 8. The aromatic isocyanate (3 mmol), amine (3.05 mmol), THF (30 mL), and DMF (3 mL) were mixed under an argon atmosphere. The reaction mixture was stirred at 20 °C for 16 hours. The solution was concentrated *in vacuo* and the residue was dissolved in the 1M NaOH (100 mL) solution and filtered to remove any insoluble material. The bisaromatic ureas were then isolated by inducing gelation through the addition of conc. HCl and filtering. The resulting gels **1** (0.96 g, 94%), **2** (0.97 g, 87%), **3** (0.80 g, 72%), **4** (1.02 g, 85%), **5** (0.95 g, 92%), **6** (0.90 g, 81%), **7** (0.78 g, 70%), **8** (0.89 g, 74%) were then washed with deionized water until neutral and dried under vacuum.

5-(3-(4-Nitrophenyl)ureido)isophthalic acid[12] **(1).** Mp 281 – 283 °C (lit. 296 – 297 °C);[12] FTIR ATR: 3366 (νN-H), 3329 (νN-H), 3120 (νC-$H_{aromatic}$), 2972 (νC-H_{alkyl}), 1720 (νC=O_{acid}), 1703 (νC=O_{acid}), 1600 (νC=O_{urea}), 1538 (νN-$O_{asymmetric}$), 1320 (νN-$O_{symmetric}$); ^{1}H NMR: (400 MHz, DMSO-d_6) δ 10.40 (s, 1H, H_e), 10.17 (s, 1H, H_g), 8.31 (d, *J* 1.5 Hz, 2H, H_i), 8.19 (AA'XX', 2H, H_b), 8.11 (t, *J* 1.5 Hz, 1H, H_k), 7.72 (AA'XX', 2H, H_c); ^{13}C{H} NMR:

(100 MHz, DMSO-d_6) δ 166.5 (C_l), 152.3 (C_f), 146.3 (C_d), 141.2 (C_a), 140.0 (C_h), 131.9 (C_j), 125.2 (C_b), 123.7 (C_k), 122.6 (C_i), 117.5 (C_c); HRMS (ESI, m/z): calcd for $C_{15}H_{12}O_7N_3$ ($[M+H]^+$) 346.0670, found 346.0668.

5-(3-(2,6-Dimethyl-4-nitrophenyl)ureido)isophthalic acid (2). Mp 285 – 287 °C ; FTIR ATR: 3346 (νN-H), 3200 (νN-H), 3073 (νC-$H_{aromatic}$), 2973 (νC-H_{alkyl}), 1714 (νC=O_{acid}), 1691 (νC=O_{acid}) 1645 (νC=O_{urea}), 1562 (νN-$O_{asymmetric}$), 1338 (νN-$O_{symmetric}$) cm^{-1}; ^{1}H NMR: (400 MHz, DMSO-d_6) δ 13.19 (s, 2H, H_n), 9.53 (s, 1H, H_h), 8.43 (s, 1H, H_f), 8.29 (d, *J* 1.5 Hz, 2H, H_j), 8.07 (t, *J* 1.6 Hz, 1H, H_l), 8.02 (s, 2 H, H_b), 2.34 (s, 6 H, H_d); ^{13}C{H} NMR: (100 MHz, DMSO-d_6) δ 166.6 (C_m), 152.3 (C_g), 144.7 (C_a), 142.0 (C_i), 140.6 (C_e), 137.0 (C_c), 131.2 (C_k), 123.2 (C_l), 122.60 (C_j), 122.58 (C_b), 18.9 (C_d); HRMS (ESI, m/z): calcd for $C_{17}H_{16}O_7N_3$ ($[M+H]^+$) 374.0983, found 374.0982.

4,6-Dimethyl-5-(3-(4-nitrophenyl)ureido)isophthalic acid (3). Mp 286 – 288 °C; 3538 (νN-H), 3258 (νN-H), 3195(νN-H), 3053 (νC-$H_{aromatic}$), 2973 (νC-H_{alkyl}), 1691 (νC=O_{acid}), 1641 (νC=O_{urea}), 1543 (νN-$O_{asymmetric}$),1327 (νN-$O_{symmetric}$) ; ^{1}H NMR: (400 MHz, DMSO-d_6) δ 13.07 (s, 2H, H_m), 10.37 (s, 1H, $H_{e/g}$), 8.72 (s, 1H, $H_{e/g}$), 8.21 – 8.13 (m, 3H, $H_b + H_n$), 7.69 (AA'XX', 2H, H_c), 2.46 (s, 6H, H_j); ^{13}C{H} NMR: (100 MHz, DMSO-d_6) δ 168.2 (C_l), 152.8(C_f), 146.9 (C_a), 140.8 ($C_d + C_k$), 137.3(C_h), 129.7(C_i), 129.3 (C_n), 125.2 (C_b), 117.1 (C_c), 16.1 (C_j); Anal. Calcd. For $C_{17}H_{15}N_3O_7$: C, 54.69; H, 4.05; N, 11.25. Found C, 54.56; H, 4.03; N, 11.21.

5-(3-(2,6-Dimethyl-4-nitrophenyl)ureido)-4,6-dimethylisophthalic acid (4). Mp 322 – 324 °C; FTIR ATR: 3250 (νN-H), 2926 (νC-H_{alkyl}), 1689 (νC=O_{acid}), 1614 (νC=O_{urea}), 1528 (νN-$O_{asymmetric}$), 1468 (νC-C), 1436 (νC-C), 1399 (νC-C), 1347 (νN-$O_{symmetric}$), cm^{-1}; ^{1}H NMR: (400 MHz, DMSO-d_6) δ 13.05 (s, 2H, H_n), 8.57 (s, 1H, $H_{f/h}$), 8.26 (s, 1H, $H_{f/h}$), 8.12 (s, 1H, H_o), 7.98 (s, 2H, H_b), 2.48 (s, 6H, H_k), 2.36 (s, 6H, H_d); ^{13}C{H} NMR: (100 MHz, DMSO-d_6) δ 168.3 (C_m), 153.1 (C_g), 144.5 (C_a), 142.7 (C_e), 140.9 (C_l), 138.0 (C_i), 136.8 (C_c), 129.5 (C_j), 129.3 (C_o), 122.6 (C_b), 18.5 (C_d), 16.1 (C_k); HRMS (ESI, *m/z*): calcd for $C_{19}H_{20}O_7N_3$ ($[M+H]^+$) 402.1296, found 402.1294.

5-(3-(3-Nitrophenyl)ureido)isophthalic acid[13] **(5).** Mp 283 – 285 °C; FTIR ATR: 3374 (νN-H), 3088 (νC-$H_{aromatic}$), 2831 (νC-H_{alkyl}), 1727 (νC=O_{acid}), 1688 (νC=O_{acid}), 1602 (νC=O_{urea}), 1521 (νN-$O_{asymmetric}$), 1440 (νC-C), 1405 (νC-C), 1333 (νN-$O_{symmetric}$) cm^{-1}; ^{1}H NMR: (400 MHz, DMSO-d_6) δ 13.22 (s, 2H, H_o), 10.02 (s, 1H, H_g), 9.93 (s, 1H, H_i), 8.55 (appt. t, H_f, 1H), 8.31 (d, *J* 1.5 Hz, 2H, H_k), 8.10 (t, *J* 1.5 Hz, 1H, H_n), 7.82 (appt. dd, 1H, H_b), 7.75 (appt. dd, 1H, H_d), 7.57 (appt. t, *J* 8.2 Hz, 1H, H_c); ^{13}C{H} NMR: (100 MHz, DMSO-d_6) δ 166.5 (C_m), 152.6 (C_g), 148.2 (C_a), 140.9 (C_e), 140.2 (C_j), 131.8 (C_l), 130.1 (C_c), 124.2 (C_d), 123.5 (C_n), 122.6 (C_k), 116.4 (C_b), 112.0 (C_f); HRMS (ESI, m/z): calcd for $C_{15}H_{12}O_7N_3$ ($[M+H]^+$) 346.0670, found 346.0668.

5-(3-(2,6-Dimethyl-3-nitrophenyl)ureido)isophthalic acid (6). Mp 269 – 271 °C; FTIR ATR: 3260 (νN-H), 3086 (νC-$H_{aromatic}$), 2932 (νC-H_{alkyl}), 1695 (νC=O_{acid}), 1646 (νC=O_{urea}), 1518 (νN-$O_{asymmetric}$), 1439 (νC-C), 1342 (νN-$O_{symmetric}$) cm^{-1}; ^{1}H NMR: (400 MHz, DMSO-d_6) δ 9.66 (1H, s, H_p), 8.41 (s, 1H, $H_{i/k}$), 8.30 (d, *J* 1.5 Hz, 2H, H_m), 8.08 (t, *J* 1.5 Hz, 1 H, H_q), 7.75 (d, *J* 8.4 Hz, 1H, H_b), 7.35 (d, *J* 8.4 Hz, 1H, H_c), 2.33 (s, 3H, H_h), 2.32 (s, 3 H, H_e); ^{13}C{H} NMR: (100 MHz, DMSO-d_6) δ 166.7 (C_n), 153.1 (C_i), 148.7 (C_a), 142.1 (C_g), 140.8 (C_l), 137.0 (C_f), 131.7 (C_n), 130.6 (C_d), 128.1 (C_c), 123.2 (C_q), 122.6 (C_m), 121.9 (C_b), 18.8 (C_e), 14.6 (C_h); HRMS (ESI, m/z): calcd for $C_{17}H_{16}O_7N_3$ ($[M+H]^+$) 374.0983, found 374.0981.

4,6-Dimethyl-5-(3-(3-nitrophenyl)ureido)isophthalic acid (7). Mp 285 – 286 °C; FTIR ATR: 3276 (νN-H), 3087 (νC-$H_{aromatic}$), 2980, (νC-H_{alkyl}), 2929 (νC-H_{alkyl}), 2860 (νC-H_{alkyl}), 1681 (νC=O_{acid}), 1642 (νC=O_{urea}), 1528 (νN-$O_{asymmetric}$), 1464 (νC-C), 1434 (νC-C), 1378 (νC-C), 1350 (νN-$O_{symmetric}$) cm^{-1}; ^{1}H NMR: (400 MHz,DMSO-d_6) δ 13.07 (s, 2H, H_o), 9.66 (s, 1H, $H_{g/i}$), 8.54 (s, 1H, H_f), 8.21 (s, 1H, $H_{g/i}$), 8.17 (s, 1H, H_p), 7.82 – 7.69 (m, 2H, $H_b + H_d$), 7.59 – 7.50 (m, 1H, H_c), 2.47 (s, 6H, H_l). ^{13}C{H} NMR: (100 MHz, DMSO-d_6) δ 168.2 (C_n), 153.2 (C_a), 148.1 (C_h), 141.5 (C_m), 141.0(Ce), 137.4 (C_j), 130.0 (C_c), 129.7 (C_p), 129.3 (C_k), 124.1 (C_d), 116.0 (C_b), 111.9 (C_f), 16.1 (C_l). HRMS (ESI, m/z): calcd for $C_{17}H_{16}O_7N_3$ ($[M+H]^+$) 374.0983, found 374.0980.

5-(3-(2,6-Dimethyl-3-nitrophenyl)ureido)-4,6-dimethylisophthalic acid (8). Mp 312 – 314 °C; FTIR ATR: 3239 (νN-H), 3085 (νC-$H_{aromatic}$), 2980 (νC-H_{alkyl}), 2926 (νC-H_{alkyl}), 1691 (νC=O_{acid}), 1619 (νC=O_{urea}), 1522 (νN-$O_{asymmetric}$), 1469 (νC-C), 1423 (νC-C), 1379 (νN-$O_{asymmetric}$) cm^{-1}; ^{1}H NMR: (400 MHz, DMSO-d_6) δ 13.05 (s, 2H, H_r),

8.33 (s, 1H, $H_{i/k}$), 8.20 (s, 1H, $H_{i/k}$), 8.13 (s, 1H, H_q), 7.72 (d, *J* 8.4 Hz, 1H, H_b), 7.33 (d, *J* 8.4 Hz, 1H, H_c), 2.49 (s, 6H, H_l), 2.37 (s, 3H, H_h), 2.35 (s, 3H, H_e). $^{13}C\{H\}$ NMR: (100 MHz, DMSO-d_6) 168.3 (C_p), 153.8 (C_j), 148.7 (C_a), 142.1 (C_d), 141.0 (C_o), 138.1 (C_f), 137.6 (C_m), 130.6 (C_g), 129.5 (C_q), 129.2 (C_n), 128.0 (C_c), 121.7 (C_b), 18.7 (C_e), 16.1 (C_l), 14.5 (C_h). Anal. Calcd. For $C_{19}H_{19}N_3O_7$: C, 56.86; H, 4.77; N, 10.46. Found C, 56.56; H, 4.64; N, 10.21.

1,5-Bis(chloromethyl)-2,4-dimethylbenzene[28] **(9).** *m*-Xylene (86.0 g, 810.0 mmol), paraformaldehyde (55.9 g, 1.86 mol), were suspended in conc. HCl (800 mL) and glacial acetic acid (200 mL) and heated to 70 °C for 96 hours, over which time the reaction mixture turned clear, and large colorless crystals started to form. The reaction mixture was cooled to 20 °C and extracted with dichloromethane (5 × 200 mL). The combined organic phases were washed with $NaHCO_3$ solution (3 × 200 mL), water (3 × 200 mL), and brine (3 × 200 mL). The organic phase was then dried over $MgSO_4$, filtered and evaporated to dryness to yield a white crystalline solid, which was subsequently purified by crystallization from hexane (120.4 g, 73%). Mp 95 – 96 °C (lit. 95 °C);[28] FTIR ATR: 3011 (νC-$H_{aromatic}$), 2974 (νC-H_{alkyl}), 2925 (νC-H_{alkyl}), 2864 (νC-H_{alkyl}), 1618 (νC-C), 1507 (νC-C), 1450 (νC-C) cm^{-1}; ^1H NMR: (400 MHz, DMSO-d_6) δ 7.38 (s, 1H, H_f), 7.09 (s, 1H, H_e), 4.74 (s, 4H, H_a), 2.33 (s, 6H, H_d); $^{13}C\{H\}$ NMR: (100 MHz, DMSO-d_6) δ 137.8 (C_b), 133.4 (C_c), 132.7 (C_e), 131.5 (C_f), 44.6 (C_a), 17.9 (C_d);
Anal. Calcd. For $C_{10}H_{12}Cl_2$: C, 59.14; H, 5.95. Found: C, 59.33; H, 5.95.

1,5-Bis(chloromethyl)-2,4-dimethyl-3-nitrobenzene[29] **(10). 9** (10.0 g, 49.2 mmol) was added to $CHCl_3$ (80 mL) at 0 °C and conc. H_2SO_4 (75 mL) was added slowly to the vigorously stirring solution, conc. HNO_3 (14.3 mL, ρ = 1.4) was then added dropwise over 30 minutes. The reaction mixture was immediately separated, and the H_2SO_4 layer was then back extracted with $CHCl_3$ (80 mL × 1). The combined organic phases were washed with deionized water (200 mL), Na_2CO_3 solution (2M, 3 × 200 mL), and brine (3 × 200 mL). The organic phase was then dried over $MgSO_4$, filtered and evaporated to dryness to yield a white crystalline solid, which was subsequently purified by crystallization from MeOH (9.7 g, 79%). Mp 143 – 144 °C (lit. 140 – 141 °C);[29] FTIR ATR: 3036 (νC-$H_{aromatic}$), 3009 (νC-$H_{aromatic}$), 2971 (νC-H_{alkyl}), 2893 (νC-H_{alkyl}), 1518 (νN-$O_{asymmetric}$), 1452 (νC-C), 1373 (νN-$O_{symmetric}$) cm^{-1}; ^1H NMR: (400 MHz, DMSO-d_6) δ 7.72 (s, 1H, H_f), 4.86 (s, 4H, H_e), 2.25 (s, 6H, H_c); $^{13}C\{H\}$ NMR: (100 MHz, DMSO-d_6) δ 153.2 (C_a), 135.7 (C_b), 132.9 (C_f), 128.4 (C_d), 43.6 (C_e), 13.0 (C_c); Anal. Calcd. For $C_{10}H_{11}NO_2Cl_2$: C, 48.41; H, 4.47; N, 5.65. Found: C, 48.25; H, 4.39; N, 5.63.

4,6-Dimethyl-5-nitroisophthalic acid[29] **(11). 10** (8.00 g, 34.24 mmol) was added to conc. HNO_3 (200 mL, ρ = 1.4) and heated to 130 °C for 24h. **11** precipitated as a white crystalline mass upon cooling to 20 °C and was filtered, washed with cold deionized water (3 × 10 mL) and then dried (6.67 g, 86%). Mp 314 – 315 °C (lit. 294 °C);[29] FTIR ATR: 2992 (νC-H_{alkyl}), 2884(νC-H_{alkyl}), 1688 (νC=O_{acid}), 1530 (νN-$O_{asymmetric}$), 1484 (νC-C), 1421 (νC-C), 1394 (νN-$O_{symmetric}$) cm^{-1}; ^1H NMR: (400 MHz, DMSO-d_6) δ 13.56 (s, 2H, H_f), 8.39 (s, 1H, H_g), 2.41 (s, 6H, H_c); $^{13}C\{H\}$ NMR: (100 MHz, DMSO-d_6) δ 166.6 (C_e), 154.4 (C_a), 133.13 (C_g), 133.05 (C_d), 130.1(C_b), 15.1 (C_c).
HRMS (ESI, m/z): calcd for $C_{10}H_9NO_6$ ($[M-H]^+$) 238.0352, found 238.0344.

Dimethyl 4,6-dimethyl-5-nitroisophthalate[29] **(12).** Thionyl chloride (6.8 mL, 94.1 mmol) was added dropwise to a stirred suspension of **11** (4.5 g, 18.8 mmol) in MeOH (100 mL) at 0 °C under argon. The reaction mixture was stirred at 20 °C and monitored by TLC (4 : 1 EtOAc : n-hexane) analysis. The solvent was removed *in vacuo* after completion of the reaction to yield **12** as a crystalline solid (4.80 g, 95%). Mp 143 – 144 °C (lit. 143.5 – 144.5 °C);[29] FTIR ATR: 2962 (νC-H_{alkyl}), 1723 (νC=O_{ester}), 1532 (νN-$O_{asymmetric}$), 1446 (νC-C), 1435 (νC-C), 1294 (νN-$O_{symmetric}$) cm^{-1}; ^1H NMR: (400 MHz, DMSO-d_6) δ 8.40 (s, 1H, H_d), 3.89 (s, 6H, H_a), 2.44 (s, 6H, H_g); $^{13}C\{H\}$ NMR: (100 MHz, DMSO-d_6) δ 165.1 (C_b), 154.2 (C_e), 133.5 (C_c), 132.7 (C_d), 129.2 (C_f), 52.7 (C_a), 15.0 (C_g); HRMS (ESI, *m/z*): calcd for $C_{12}H_{13}NO_6Na$ ($[M+Na]^+$) 290.0635, found 290.0641.

Dimethyl 5-amino-4,6-dimethylisophthalate[29] **(13).** Pd/C (10 wt. %, 300 mg) and **12** (3.0 g, 11.2 mmol) were suspended in MeOH (30 mL) under a hydrogen atmosphere. The suspension was stirred for 3 hours at 20 °C, filtered through a bed of celite and the solvent removed *in vacuo* to isolate the desired target material as a

white solid (2.60 g, 98%). Mp 95 – 96 °C (lit. 95.5 – 97 °C);[43] FTIR ATR: 3454 (νN-H), 3378 (νN-H), 3004 (νC-$H_{aromatic}$), 2952 (νC-H_{alkyl}), 2842 (νC-H_{alkyl}), 1712 (νC=O_{ester}), 1432 (νC-C), 1403 (νC-C) cm^{-1}; ^{1}H NMR: (400 MHz, DMSO-d_6) δ 7.37 (s, 1H, H_d), 5.09 (s, 2H, H_h), 3.80 (s, 6H, H_a), 2.29 (s, 6H, H_g); ^{13}C{H} NMR: (100 MHz, DMSO-d_6) δ 167.9 (C_b), 146.4 (C_e), 128.1(C_f), 124.2 (C_c), 118.4(C_d), 51.9 (C_a), 14.6 (C_g); HRMS (ESI, m/z): calcd for $C_{12}H_{15}NO_4$ ([M+H]$^+$) 238.1074, found 238.1070.

5-Amino-4,6-dimethylisophthalic acid[43] **(14).** NaOH (1.28 g, 32.0 mmol) was added to a stirred solution of **13** (3.45 g, 14.5 mmol) in MeOH (50 mL) and water (10 mL). The reaction mixture was maintained under reflux for 3 hours under argon. The reaction mixture was monitored by TLC (9 :1 EtOAc : MeOH) analysis and upon completion was cooled to 20 °C and acidified with 6M HCl, at pH 4 a large volume of white precipitate is formed, filtered, and dried *in vacuo* (2.17 g, 71%). Mp 308 – 310 °C (lit. 305 – 306 °C);[43] FTIR ATR: 3495 (νN-H), 3413 (νN-H), 2869 (νC-H_{alkyl}), 2815 (νC-H_{alkyl}), 1671 (νC=O_{acid}), 1488 (νC-C), 1442 (νC-C), 1427 (νC-C), 1410 (νC-C) cm^{-1}; ^{1}H NMR: (400 MHz, DMSO-d_6) δ 12.65 (s, 2H, H_a), 7.39 (s, 1H, H_d), 4.95 (s, 2H, H_h), 2.30 (s, 6H, H_g); ^{13}C{H} NMR: (100 MHz, DMSO-d_6) δ 169.4 (C_b), 146.2 (C_e), 129.1 (C_f), 123.8 (C_c), 118.8 (C_d), 14.66 (C_g); Anal. Calcd. For $C_{10}H_{11}NO_4$: C, 57.41; H, 5.30; N, 6.69. Found C, 57.26; H, 5.28; N, 6.65.

2-Isocyanato-1,3-dimethyl-4-nitrobenzene (15) To a solution of phosgene (47.2 mL, 66.2 mmol, 15 wt. % in toluene) at 0 °C, a solution of **17** (5.0 g, 30.1 mmol) in anhydrous THF was added dropwise over the course of 1 hour at 0 – 10 °C and allowed to react for a further 24 hours. The volatiles were removed *in vacuo* and the yellow crystalline solid was stored at -10 °C under an argon atmosphere (5.78 g, >99%). Mp 45 – 46 °C; FTIR ATR: 3092 (νC-$H_{aromatic}$), 2990 (νC-H_{alkyl}), 2955 (νC-H_{alkyl}), 2928 (νC-H_{alkyl}), 2862 (νC-H_{alkyl}), 2272 (νNCO), 1506 (νN-$O_{asymmetric}$), 1455 (νC-C), 1443 (νC-C), 1346 (νN-$O_{symmetric}$) cm^{-1}; ^{1}H NMR: (400 MHz, $CDCl_3$) δ 7.64 (d, *J* 8.4 Hz, 1H, H_b), 7.18 (d, *J* 8.4 Hz, 1H, H_c), 2.52 (s, 3H, H_i), 2.43 (s, 3H, H_e); ^{13}C{H} NMR: (100 MHz, $CDCl_3$) δ 149.0 (C_a), 138.8 (C_h), 133.4 (C_f), 128.1 (C_d), 128.1 (C_c), 124.8 (C_g), 121.3 (C_b), 19.4 (C_e), 15.2 (C_i);
Anal. Calcd. For $C_9H_8N_2O_3$: C, 56.25; H, 4.20; N, 14.57. Found C, 56.16; H, 4.16; N, 14.50.

2-Isocyanato-1,3-dimethyl-5-nitrobenzene (16). To a solution of phosgene (42.5 mL, 59.6 mmol, 15 wt. % in toluene) at 0 °C, a solution of **18** (4.5 g, 27.1 mmol) dissolved in anhydrous THF was added dropwise over the course of 1 hour at 0 – 10 °C and allowed to react for a further 24 hours. The volatiles were removed *in vacuo* and the yellow crystalline solid was stored at -10 °C under an argon atmosphere (5.20 g, > 99%). Mp 90 – 91 °C; FTIR ATR: 3083 (νC-$H_{aromatic}$), 2964 (νC-H_{alkyl}), 2928 (νC-H_{alkyl}), 2852 (νC-H_{alkyl}), 2263 (νNCO), 1512 (νN-$O_{asymmetric}$), 1457 (νC-C), 1442(νC-C), 1425 (νC-C), 1342 (νN-$O_{symmetric}$) cm^{-1}; ^{1}H NMR: (400 MHz, DMSO-d_6) δ 7.9 (s, 2H, H_b), 2.4 (s, 6H, H_d); ^{13}C{H} NMR: (100 MHz, DMSO-d_6) δ 144.6 (C_a), 137.6 (C_e), 134.4 (C_c), 125.7 (C_f), 123.3 (C_b), 19.0 (C_d); Anal. Calcd. For $C_9H_8N_2O_3$: C, 56.25; H, 4.20; N, 14.57. Found C, 56.07; H, 4.24; N, 14.28.

2,6-Dimethyl-3-nitroaniline[44] **(17).** 2,6-Dimethylaniline (10.0 g, 82.5 mmol) was dissolved in conc. H_2SO_4 (80 mL), conc. HNO_3 (4.1 mL, ρ = 1.4) was added dropwise keeping the temperature at 10 – 15 °C. The reaction mixture was stirred for 1 hour and then poured into ice-water and made basic (pH 10) with 6M NaOH solution without the temperature of the mixture exceeding 25 °C. The yellow precipitate was collected and recrystallized from methanol to give yellow crystals (11.4 g, 83%). Mp 81 – 82 °C (lit. 81 – 82 °C);[45] FTIR ATR: 3422 (νN-H), 3350 (νN-H), 3100 (νC-$H_{aromatic}$), 2982 (νC-H_{alkyl}), 2951 (νC-H_{alkyl}), 2919 (νC-H_{alkyl}), 2851 (νC-H_{alkyl}), 1635 (νN-H_{bend}), 1601 (νC-C), 1514 (νN-$O_{asymmetric}$), 1481 (νC-C), 1460 (νC-C), 1434 (νC-C), 1423 (νC-C), 1349 (νN-$O_{symmetric}$), 1322 (νC-N) cm^{-1}; ^{1}H NMR: (400 MHz, DMSO-d_6) δ 6.98 (d, *J* 8.2 Hz, 1H, H_i), 6.93 (d, *J* 8.2 Hz, 1H, H_h), 5.22 (s, 2H, H_e), 2.15 (appt. s, 6H, $H_{c/g}$); ^{13}C{H} NMR: (100 MHz, DMSO-d_6) δ 149.6 (C_a), 146.0 (C_d), 127.4 (C_i), 125.7 (C_f), 113.3(C_b), 110.6 (C_h), 18.3 ($C_{c/g}$), 13.0 ($C_{c/g}$); HRMS (ESI, m/z): $C_8H_{11}N_2O_2$ ([M+H]$^+$) 167.0815, found 167.0812.

2,6-Dimethyl-4-nitroaniline[46] **(18). 20** (10.0 g, 31.2 mmol), conc. H_2SO_4 (100 mL) and deionized water (10 mL) were mixed together and stirred for 24 hours, after which the reaction mixture diluted with water (250 mL) and

made basic with NH_4OH (30% NH_3) solution and filtered. The yellow precipitate was then recrystallized from ethanol:water 50:50 to give yellow crystals (4.20 g, 81%). Mp 162 – 163 °C (lit. 163.5 – 164.5 °C);[46] FTIR ATR: 3492 (νN-H), 3390 (νN-H), 2984 (νC-H_{alkyl}), 2940 (νC-H_{alkyl}), 2915 (νC-H_{alkyl}), 2852 (νC-H_{alkyl}), 1626 (νN-H_{bend}), 1595 (νC-C), 1486 (νN-$O_{asymmetric}$), 1463 (νC-C), 1324 (νN-$O_{symmetric}$) cm^{-1}; ^1H NMR: (400 MHz, DMSO-d_6) δ 7.77 (s, 2H, H_b), 6.13 (s, 2H, H_f), 2.15 (s, 6H, H_d); $^{13}C\{H\}$ NMR: (100 MHz, DMSO-d_6) δ 152.0 (C_a), 135.2 (C_e), 124.1 (C_b), 120.0 (C_c), 17.7 (C_d); HRMS (ESI, m/z): calcd for $C_8H_{11}N_2O_2$ ($[M+H]^+$) 167.0815, found 167.0814.

N-(2,6-Dimethylphenyl)-4-methylbenzenesulfonamide[46] **(19).** 2,6-Dimethylaniline (20.00 g, 165.04 mmol), *p*-toluenesulfonyl chloride (34.61 g, 181.54 mmol) were suspended in pyridine (75 mL) and heated to 120 °C for 4 hours. The reaction mixture was cooled to 20 °C poured into 2M HCl (750 mL) and extracted with ethyl acetate (3 × 200 mL). The combined organic phases were washed with water (3 × 200 mL) and brine (3 × 200 mL). The organic phase was then dried over $MgSO_4$, filtered and evaporated to dryness to yield an off-white solid, which was subsequently purified by crystallization from ethanol (30.10 g, 66%). Mp = 135 – 137 °C (lit. 136.5 – 137.5 °C);[46] FTIR ATR: 3281 (νN-H), 3038 (νC-$H_{aromatic}$), 2971 (νC-H_{alkyl}), 2925 (νC-H_{alkyl}), 2859 (νC-H_{alkyl}), 1597 (νC-C), 1472 (νSO_2), 1154 (νSO_2) cm^{-1}; ^1H NMR: (400 MHz, DMSO-d_6) 9.25 (s, 1H, H_f), 7.58 – 7.51 (AA'XX', 2H, H_h), 7.39 – 7.32 (AA'XX', 2 H, H_i), 7.05 (dd, *J* 8.7, 6.0 Hz, 1H, H_d), 7.01 – 6.97 (m, 2H, H_c), 2.38 (s, 3H, H_k), 1.94 (s, 6H, H_a); $^{13}C\{H\}$ NMR: (100 MHz, DMSO-d_6) δ 142.8 (C_j), 139.2 (C_g), 137.7 (C_b), 133.4 (C_e), 129.6 (C_i), 128.4 (C_c), 127.2 (C_d), 126.4 (C_i), 21.0 (C_k), 18.5 (C_a); HRMS (ESI, m/z): calcd for $C_{15}H_{17}NO_2S$ ($[M+H]^+$) 276.1053, found 276.1051.

N-(2,6-Dimethyl-4-nitrophenyl)-4-methylbenzenesulfonamide[46] **(20).** To a solution of conc. HNO_3 (20.0 mL, ρ = 1.52 gmL^{-1}) and deionized water (150 mL) was added **19** (20.0 g, 72.6 mmol), glacial acetic acid (150 mL) and $NaNO_2$ (501 mg, 7.3 mmol). The suspension was heated to 140 °C for 2 hours, over which time the reaction mixture turned clear after some time large colourless crystals started to form. The reaction mixture was cooled to 20 °C, and deionized water (300 mL) was added to precipitate the desired product, which was subsequently purified by crystallization from ethanol (16.8 g, 72%). Mp 165 – 167 °C (lit. 167 – 168 °C);[46] FTIR ATR: 3265 (νN-H), 3081 (νC-$H_{aromatic}$), 2929 (νC-H_{alkyl}), 2857 (νC-H_{alkyl}), 1597 (νC-C), 1589 (νC-C), 1510 (νN-$O_{asymmetric}$), 1494 (νSO_2), 1294 (νN-$O_{symmetric}$), 1155 (νSO_2), cm^{-1}; ^1H NMR: (400 MHz, DMSO-d_6) δ 9.73 (s, 1H, H_f), 7.92 (s, 2H, H_c), 7.57 (AA'XX', 2H, H_h), 7.39 (AA'XX', 2H, H_i), 2.39 (s, 3H, H_k), 2.07 (s, 6H, H_a);$^{13}C\{H\}$ NMR: (100 MHz, DMSO-d_6) δ 145.5 (C_d), 143.4 (C_j), 139.9 (C_e), 139.7 (C_b), 138.7 (C_g), 129.9 (C_i), 126.4 (C_h), 123.0 (C_c), 21.0 (C_k), 18.6 (C_a); HRMS (ESI, m/z): calcd for $C_{15}H_{16}N_2O_4S$ ($[M-H]^+$) 319.0758, found 319.0744.

Crystals of **10** and **12** were mounted under Paratone-N oil and flash cooled to 100 K under nitrogen in an Oxford Cryosystems Cryostream. Single-crystal X-ray intensity data were collected using a Rigaku XtaLAB Synergy diffractometer (Cu K*α* radiation (λ = 1.54180 Å)). The data were reduced within the CrysAlisPro software.[47] The structures were solved using the program Superflip[48] and all non-hydrogen atoms located. Least-squares refinement against *F* was carried out using the *CRYSTALS* suite of programs.[49] The non-hydrogen atoms were refined anisotropically. All the hydrogen atoms were located in difference Fourier maps, then placed geometrically with a C-H distance of 0.95 Å and a U_{iso} of ~1.2 times the value of U_{eq} of the parent C atom. The hydrogen atoms were then refined with riding constraints.

Acknowledgments

The authors would like to acknowledge financial support from EPSRC and Kinectrics UK Ltd (PhD studentship for ADOD). This study was also supported by Dstl (contract DSTLX1000116213R, PhD studentship for AGG). In

addition, the University of Reading (EPSRC-Doctoral Training Grant) is acknowledged for granting access to instrumentation in the Chemical Analysis Facility. We thank Mr. Nick Spencer (University of Reading) for his help in collecting the single-crystal X-ray diffraction data.

Supplementary Material

Characterization of compounds **1**-**20**, ^{1}H NMR and ^{13}C{H} NMR spectra, additional rheological data, and solid-state structure of compound **10** and **12**.

References

1. Lehn, J.-M.; Mascal, M.; Decian, A.; Fischer, J. *J. Chem. Soc. Chem. Commun.* **1990**, 479–481. https://doi.org/10.1039/c39900000479
2. Lehn, J.-M. *Angew. Chemie Int. Ed.* **2015**, *54*, 3276–3289. https://doi.org/10.1002/anie.201409399
3. Müller-Dethlefs, K.; Hobza, P. *Chem. Rev.* **2000**, *100*, 143–167. https://doi.org/10.1021/cr9900331
4. Lehn, J.-M. *Science.* **2002**, *295*, 2400–2403. https://doi.org/10.1126/science.1071063
5. van Gorp, J. J.; Vekemans, J. A. J. M.; Meijer, E. W. *Chem. Commun.* **2004**, *4*, 60–61. https://doi.org/10.1039/b312407j
6. Etter, M. C.; Zia-Ebrahimi, M.; Urbañczyk-Lipkowska, Z.; Panunto, T. W. *J. Am. Chem. Soc.* **1990**, *112*, 8415–8426. https://doi.org/10.1021/ja00179a028
7. Etter, M. C.; Panunto, T. W. *J. Am. Chem. Soc.* **1988**, *110*, 5896–5897. https://doi.org/10.1021/ja00225a049
8. van Esch, J.; Schoonbeek, F.; de Loos, M.; Kooijman, H.; Spek, A. L.; Kellogg, R. M.; Feringa, B. L. *Chem. - A Eur. J.* **1999**, *5*, 937–950. https://doi.org/10.1002/(SICI)1521-3765(19990301)5:3<937::AID-CHEM937>3.0.CO;2-0
9. van der Laan, S.; Feringa, B. L.; Kellogg, R. M.; van Esch, J. *Langmuir* **2002**, *18*, 7136–7140. https://doi.org/10.1021/la025561d
10. Mohmeyer, N.; Schmidt, H. W. *Chem. - A Eur. J.* **2007**, *13*, 4499–4509. https://doi.org/10.1002/chem.200601154
11. Baker, B. C.; Acton, A. L.; Stevens, G. C.; Hayes, W. *Tetrahedron* **2014**, *70*, 8303–8311. https://doi.org/10.1016/j.tet.2014.09.017
12. Rodríguez-Llansola, F.; Escuder, B.; Miravet, J. F.; Hermida-Merino, D.; Hamley, I. W.; Cardin, C. J.; Hayes, W. *Chem. Commun.* **2010**, *46*, 7960–7962. https://doi.org/10.1039/c0cc02338h
13. Wood, D. M.; Greenland, B. W.; Acton, A. L.; Rodríguez-Llansola, F.; Murray, C. A.; Cardin, C. J.; Miravet, J. F.; Escuder, B.; Hamley, I. W.; Hayes, W. *Chem. - A Eur. J.* **2012**, *18*, 2692–2699. https://doi.org/10.1002/chem.201102137
14. Kishikawa, K.; Nakahara, S.; Nishikawa, Y.; Kohmoto, S.; Yamamoto, M. *J. Am. Chem. Soc.* **2005**, *127*,

2565–2571.
https://doi.org/10.1021/ja046100c
15. Vonau, F.; Suhr, D.; Aubel, D.; Bouteiller, L.; Reiter, G.; Simon, L. *Phys. Rev. Lett.* **2005**, *94*, 1–4.
https://doi.org/10.1103/PhysRevLett.94.066103
16. Moon, K.; Kaifer, A. E. *J. Am. Chem. Soc.* **2004**, *126*, 15016–15017.
https://doi.org/10.1021/ja045587m
17. Zhu, C.; Tang, H.; Yang, K.; Wu, X.; Luo, Y.; Wang, J.; Li, Y. *Catal. Commun.* **2020**, *135*, 105837.
https://doi.org/10.1016/j.catcom.2019.105837
18. Brunsveld, L.; Folmer, B. J. B.; Meijer, E. W.; Sijbesma, R. P. *Chem. Rev.* **2001**, *101*, 4071–4097.
https://doi.org/10.1021/cr990125q
19. Gunnlaugsson, T.; Glynn, M.; Tocci (née Hussey), G. M.; Kruger, P. E.; Pfeffer, F. M. *Coord. Chem. Rev.* **2006**, *250*, 3094–3117.
https://doi.org/10.1016/j.ccr.2006.08.017
20. Custelcean, R. *Chem. Commun.* **2008**, 295–307.
https://doi.org/10.1039/B708921J
21. Isare, B.; Pembouong, G.; Boué, F.; Bouteiller, L. *Langmuir* **2012**, *28*, 7535–7541.
https://doi.org/10.1021/la300887p
22. Norouzi, M.; Nazari, B.; Miller, D. W. *Drug Discov. Today* **2016**, *21*, 1835–1849.
https://doi.org/10.1016/j.drudis.2016.07.006
23. Bhattacharya, S.; Krishnan-Ghosh, Y. *Chem. Commun.* **2001**, 185–186.
https://doi.org/10.1039/b007848o
24. Okesola, B. O.; Smith, D. K. *Chem. Soc. Rev.* **2016**, *45*, 4226–4251.
https://doi.org/10.1039/C6CS00124F
25. Chen, L.; Raeburn, J.; Sutton, S.; Spiller, D. G.; Williams, J.; Sharp, J. S.; Griffiths, P. C.; Heenan, R. K.; King, S. M.; Paul, A.; Furzeland, S.; Atkins, D.; Adams, D. J. *Soft Matter* **2011**, *7*, 9721.
https://doi.org/10.1039/c1sm05827d
26. Patterson, A. K.; Smith, D. K. *Chem. Commun.* **2020**, *56*, 11046–11049.
https://doi.org/10.1039/D0CC03962D
27. Fleming, S.; Debnath, S.; Frederix, P. W. J. M.; Tuttle, T.; Ulijn, R. V. *Chem. Commun.* **2013**, *49*, 10587–10589.
https://doi.org/10.1039/c3cc45822a
28. Gerisch, M.; Krumper, J. R.; Bergman, R. G.; Tilley, T. D. *J. Am. Chem. Soc.* **2001**, *123*, 5818–5819.
https://doi.org/10.1021/ja005857a
29. Hopff, H.; Maggi, A.; Manukian, B. K. *Helv. Chim. Acta* **1961**, *44*, 367–379.
https://doi.org/10.1002/hlca.19610440205
30. Murata, K.; Aoki, M.; Suzuki, T.; Harada, T.; Kawabata, H.; Komori, T.; Ofaseto, F.; Ueda, K.; Shinkai, S. *J. Am. Chem. Soc.* **1994**, *116*, 6664–6676.
https://doi.org/10.1021/ja00094a023
31. Adams, D. J.; Butler, M. F.; Frith, W. J.; Kirkland, M.; Mullen, L.; Sanderson, P. *Soft Matter* **2009**, *5*, 1856–1862.
https://doi.org/10.1039/b901556f
32. Rutgeerts, L. A. J.; Soultan, A. H.; Subramani, R.; Toprakhisar, B.; Ramon, H.; Paderes, M. C.; De Borggraeve, W. M.; Patterson, J. *Chem. Commun.* **2019**, *55*, 7323–7326.
https://doi.org/10.1039/C9CC02927C

33. Talebian, S.; Mehrali, M.; Taebnia, N.; Pennisi, C. P.; Kadumudi, F. B.; Foroughi, J.; Hasany, M.; Nikkhah, M.; Akbari, M.; Orive, G.; Dolatshahi-Pirouz, A. *Adv. Sci.* **2019**, *6*, 1801664.
https://doi.org/10.1002/advs.201801664
34. Wang, H.; Biswas, S. K.; Zhu, S.; Lu, Y.; Yue, Y.; Han, J.; Xu, X.; Wu, Q.; Xiao, H. *Nanomaterials* **2020**, *10*, 112.
https://doi.org/10.3390/nano10010112
35. Liao, H.; Guo, X.; Wan, P.; Yu, G. *Adv. Funct. Mater.* **2019**, *29*, 1904507.
https://doi.org/10.1097/01.tp.0000581312.52804.72
36. Li, H.; Lv, T.; Sun, H.; Qian, G.; Li, N.; Yao, Y.; Chen, T. *Nat. Commun.* **2019**, *10*, 536.
https://doi.org/10.1038/s41467-019-08320-z
37. Gao, G.; Du, G.; Sun, Y.; Fu, J. *ACS Appl. Mater. Interfaces* **2015**, *7*, 5029–5037.
https://doi.org/10.1021/acsami.5b00704
38. Escuder, B.; LLusar, M.; Miravet, J. F. *J. Org. Chem.* **2006**, *71*, 7747–7752.
https://doi.org/10.1021/jo0612731
39. Tang, C.; Smith, A. M.; Collins, R. F.; Ulijn, R. V.; Saiani, A. *Langmuir* **2009**, *25*, 9447–9453.
https://doi.org/10.1021/la900653q
40. Avrami, M. *J. Chem. Phys.* **1939**, *7*, 1103–1112.
https://doi.org/10.1063/1.1750380
41. Moffat, J. R.; Smith, D. K. *Chem. Commun.* **2008**, *44*, 2248–2250.
https://doi.org/10.1039/b801913d
42. Adams, D. J.; Morris, K.; Chen, L.; Serpell, L. C.; Bacsa, J.; Day, G. M. *Soft Matter* **2010**, *6*, 4144–4156.
https://doi.org/10.1039/c0sm00409j
43. de Diesbach, H.; Chardonnens, L. *Helv. Chim. Acta* **1924**, *7*, 614–618.
https://doi.org/10.1002/hlca.19240070175
44. Bergman, J.; Sand, P. *Tetrahedron* **1990**, *46*, 6085–6112.
https://doi.org/10.1016/S0040-4020(01)87932-1
45. Suzuki, H.; Maruyama, K.; Goto, R. *Bull. Chem. Soc. Jpn.* **1965**, *38*, 1590–1595.
https://doi.org/10.1246/bcsj.38.1590
46. Wepster, B. M. *Recl. des Trav. Chim. des Pays-Bas* **1954**, *73*, 809–818.
https://doi.org/10.1002/recl.19540731004
47. CrysAlis PRO. Rigaku OD (2019). Rigaku Oxford Diffraction Ltd, Yarnton, Oxfordshire, England.
48. Palatinus, L.; Chapuis, G. *J. Appl. Crystallogr.* **2007**, *40*, 786–790.
https://doi.org/10.1107/S0021889807029238
49. Betteridge, P. W.; Carruthers, J. R.; Cooper, R. I.; Prout, K.; Watkin, D. J. *J. Appl. Crystallogr.* **2003**, *36*, 1487–1487.
https://doi.org/10.1107/S0021889803021800